Photochemistry and Photobiology, 2006, 82: 626–634

Photosensitizers Derived from 13^2-Oxo-methyl Pyropheophorbide-a: Enhanced Effect of Indium(III) as a Central Metal in *In Vitro* and *In Vivo* Photosensitizing Efficacy

Andrew Rosenfeld[1], Janet Morgan[2], Lalit N. Goswami[1], Tymish Ohulchanskyy[3], Xiang Zheng[1], Paras N. Prasad[3], Allan Oseroff[2] and Ravindra K. Pandey*[1,3,4]

[1]Photodynamic Therapy Center, Roswell Park Cancer Institute, Buffalo, NY
[2]Department of Dermatology, Roswell Park Cancer Institute, Buffalo, NY
[3]Institute of Lasers, Photonics and Biophotonics, State University of New York, Buffalo, NY
[4]Department of Nuclear Medicine, Roswell Park Cancer Institute, Buffalo, NY

Received 29 September 2005; accepted 3 November 2005; published online 3 November 2005 DOI: 10.1562/2005-09-29-RA-704

ABSTRACT

The effects of an additional keto group on absorption wavelength and the corresponding metal complexes Zn(II), Cu(II) In(III) on singlet oxygen production and photodynamic efficacy were examined among the alkyl ether analogs of pyropheophorbide-a. For the preparation of the desired photosensitizers, the methyl 13^2-oxo-pyropheophorbide-a obtained by reacting methyl pyropheophorbide-a with aqueous LiOH-THF was converted into a series of alkyl ether analogs. These compounds were evaluated for photophysical properties and *in vitro* (by means of the MTT assay and intracellular localization in RIF cells) and *in vivo* (in C3H mice implanted with RIF tumors) photosensitizing efficacy. Among the alkyl ether derivatives, the methyl 3-decyloxyethyl-3-devinyl-13^2-oxo-pyropheophorbide-a was found to be most effective and the insertion of In(III) into this analog further enhanced its *in vitro* and *in vivo* photosensitizing efficacy. Fluorescence microscopy showed that, in contrast to the hexyl and dodecyl ether derivatives of HPPH (which localize in mitochondria and lysosomes, respectively), the diketo-analogs and their In(III) complexes localized in Golgi bodies. The preliminary *in vitro* and *in vivo* results suggest that, in both free-base and metalated analogs, the introduction of an additional keto group at the five-member exocyclic ring in pyropheophorbide-a diminishes its photosensitizing efficacy. This may be due to a shift in subcellular localization from mitochondria to the Golgi bodies. The further introduction of In(III) enhances photoactivity, but not by shifting the localization of the photosensitizer.

INTRODUCTION

Photodynamic therapy (PDT) of cancer is based on the administration of a photosensitizer that accumulates or is retained preferentially in tumor tissues (1,2), followed by illumination of the tumor with light matching the absorption maximum of the photosensitizer. Photochemical reactions lead primarily to the conversion of molecular oxygen ($^3O_2$) into singlet oxygen ($^1O_2$) (type II mechanism), which is believed to be a key cytotoxic agent that destroys the tumor (3). Since the worldwide approval of Photofrin® for treatment of a variety of tumors, efforts continue to develop photosensitizers with improved selectivity and longer wavelength absorption (4,5). Absorption peaks at longer wavelengths are desirable for a greater optical penetration depth of the excitation light during treatment (6,7). Chlorins and bacteriochlorins possessing a ring system fused to a porphyrin skeleton have red-shifted absorption peaks due to extended conjugation, which makes them potential candidates for PDT (4,5). Certain chlorins containing conjugated exocyclic systems—pheophorbides (8), benzochlorins (9), purpurins (10), purpurinimides (11) and bacteriopurpurinimides (12)—have been reported as effective photosensitizers. A further red shift can also be achieved by introducing electron-withdrawing groups (*e.g.* –CHO or –C=O) at an appropriate position(s) in the porphyrin skeleton (13). Other important considerations when designing a potential PDT agent are the influence of added groups on the lipophilicity of the molecule, which can affect pharmacokinetic and pharmacodynamic properties, such as clearance of the photosensitizer(s) from the system including the tumor (14,15). In previous SAR and QSAR studies involving a variety of chlorin (16–18) and bacteriochlorin-based (19,20) photosensitizers, we observed that the overall lipophilicity of the molecule plays an important role in *in vivo* activity. It has also been reported that the presence of a central metal in phthalocyanines and certain porphyrin-chlorin systems influences the formation of reactive oxygen species (ROS) (21), the rate of photobleaching and the mechanism of tumor destruction (22). Another characteristic that influences the photodynamic efficacy of a photosensitizer is its site(s) of localization (23–27). Generally, the photosensitizers that localize in mitochondria were more effective than those localizing in lysosomes or other organelles (28).

So far, two main synthetic chemistry approaches have been used to develop long wavelength–absorbing photosensitizers: the first involves modifying the naturally occurring chlorin and bacteriochlorin systems and the second involves preparing chlorins and bacteriochlorins or other porphyrin-based photosensitizers from pyrroles in a multistep synthetic process (4). Our approach at Roswell Park Cancer Institute (Buffalo, NY) has focused on

*Corresponding author email: ravindra.pandey@roswellpark.org (Ravindra K. Pandey)

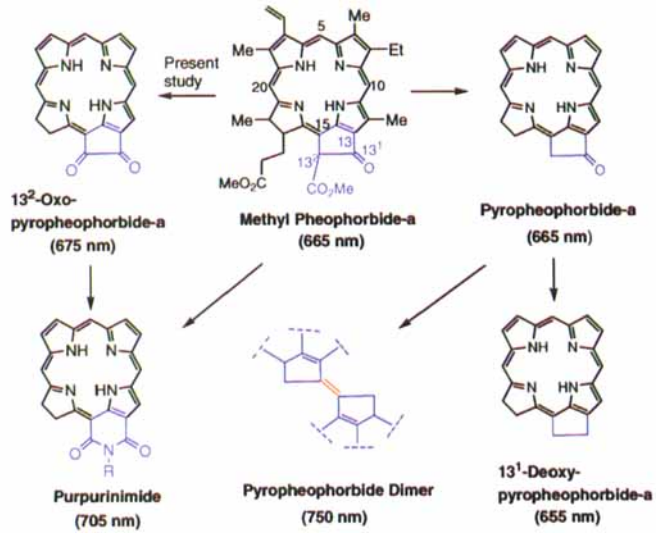

Figure 1. Substitution and structural modifications of the exocyclic ring in methyl pheophorbide-a.

isolating chlorophyll-a and bacteriochlorophyll-a from natural sources and using them as substrates for further modifications. These modifications led to certain novel structures, pyropheophorbide-a, purpurinimide and bacteriopurpurinimide, with fused imide ring systems exhibiting long wavelength absorption at 660, 700 and 800 nm, respectively (4,5). These photosensitizers are currently at various stages of clinical and preclinical trials and the initial results are quite promising.

In our efforts to establish the structure-activity relationship among tetrapyrrole-based compounds, we observed that, besides overall lipophilicity, the presence and position of the substituents also play very important roles in *in vivo* efficacy (29,30). Furthermore, the effect of substituents is similar in a particular family of compounds but varies from one system to another. For example, on the basis of SAR and QSAR studies, the alkyl ethers of pyropheophorbide showed a parabolic relationship between efficacy and lipophilicity, whereas in purpurinimide and bacteriopurpurinimide analogs a linear relationship was observed. In another study it was observed that replacement of the vinyl group with a formyl substituent at position-3 of pyropheophorbide-a enhanced its photosensitizing efficacy (13), whereas no significant difference was observed in the purpurinimide system. Again, in HPPH the reduction of the keto group at position 13^1 (deoxy analog; Fig. 1) produced a blue shift in its electronic absorption spectrum without showing any significant difference in photosensitizing ability. However, in both pyropheophorbide-a and purpurinimide systems the introduction of the alkyl ether groups at position-3 produced a significant increase in *in vivo* efficacy.

In the present study, we were interested in investigating the effect of an additional keto group at position 13^2 of a series of the alkyl ether analogs of pyropheophorbide-a and their metal complexes. The presence of an additional keto group in the five-member exocyclic ring also provides an opportunity to extend conjugation by preparing the corresponding dimers with C=C linkages (31) or by reacting them with a series of aromatic structures containing diamino functionalities (32).

The present article is focused on the synthesis, photophysical properties, *in vitro*/*in vivo* photosensitizing efficacy and intracellular localization characteristics of free-base and certain metallated analogs of methyl-13^2-oxopyropheophorbide-a.

MATERIALS AND METHODS

Chemistry. The synthetic intermediates and the final products were characterized by NMR (Brucker 400 MHz) and mass spectrometry (HRMS) analyses. The NMR data are expressed in δ ppm. The HRMS analyses were performed at the Mass Spectrometry Facility, Michigan State University (East Lansing, MI). All photophysical experiments were performed using spectroscopic-grade solvents. The reactions were monitored by TLC and/or by spectrophotometer. Column chromatography was performed over either Silica Gel 60 (70–230 mesh, Analtech) or neutral Alumina (Brockmann grade III, 50 mesh). UV-visible spectra were recorded on a Varian Cary 50 Bio UV-visible spectrophotometer, using dichloromethane as the solvent.

General experimental procedure. Methyl 13^2-oxopyropheophorbide-a **3**: Pyropheophorbide-a methyl ester (200 mg; 0.364 mmol) was dissolved in 25 mL THF in a 100 mL reaction flask. Lithium hydroxide (1.2 g) dissolved in 5 mL water and 15 mL methanol was added to the reaction flask. The mixture was stirred vigorously for 3 h. The reaction mixture was then concentrated at reduced pressure and neutralized with acetic acid. It was then extracted with dichloromethane. The organic layer was separated, washed with water (3 × 100 mL) and dried over sodium sulfate. The solvent was removed and the residue dissolved in dichloromethane and treated with diazomethane to convert the carboxylic acid back to methyl ester. The reaction product (a brown solid) was obtained after chromatographic purification on a silica gel column with 4% acetone/dichloromethane as an eluant and crystallization from dichloromethane-hexane (Yield = 160 mg, 78%). Results of ^{1}HNMR (400 MHz, $CDCl_3$) were as follows: δ 9.80(s, 1H, meso-H); 9.75 (s, 1H, meso-H); 9.73 (s, 1H, meso-H); 8.14 (m, 1H, $\underline{CH}$=CH_2); 6.40–6.30 (dd, 2H, CH=$\underline{CH_2}$); 5.20 (m, 1H, 17-H); 4.75 (m, 1H, 18-H); 3.85 (s, ^{3}H, $CO_2\underline{Me}$); 3.75 (q, 2H, $\underline{CH_2}CH_3$); 3.65, 3.55 and 3.30 (each s, ^{3}H, ring-CH_3); 2.88 (m, 1H, $CH_2\underline{CH}CO_2Me$); 2.75 (m, 1H, $CH_2\underline{CH}CO_2Me$); 2.45–2.31 (m, 2H, $\underline{CH_2}CH_2CO_2Me$); 1.95 (d, ^{3}H, 18-$CH_3$); 1.75 (t, ^{3}H, $CH_2\underline{CH_3}$); 0.50 (s, 1H, NH) and –2.40 (s, 1H, NH). The HRMS for $C_{34}H_{34}N_4O_4$ was calculated as 562.2580 and observed to be 563.2661(MH^+).

General procedure for preparation of alkyl ether derivatives. Pyrodione **3** (100 mg, 0.178 mmol) was placed in a dry flask under nitrogen, which was then sealed with a rubber septum. Five mL of 30% HBr/CH_3COOH was added to the flask via a syringe and the resultant mixture was stirred for 1.5 h. Excess HBr and acetic acid were removed using a high-pressure vacuum. The resulting residue was dissolved in dry dichloromethane (10 mL). Anhydrous anhydrous K_2CO_3 (1 g) and excess desired alcohol (2 mL) were added and the mixture was stirred under nitrogen for 2 h. The mixture was then diluted with dichloromethane (40 mL) and washed with water (3 × 20 mL); the organic layer was separated, dried over anhydrous sodium sulfate and concentrated. The excess alcohol was removed by vacuum distillation. The alkyl ethers were obtained as brown solids after elution from a silica chromatography column with 5% acetone-dichloromethane as the eluant. Yields of the desired products ranged from 72% to 83%.

Methyl 3-(1′-methyloxyethyl)-3-devinyl-13^2-oxopyropheophorbide-a (**7**): This compound was prepared from the pyrodione **3** (100.0 mg, 0.178 mmol) and an excess of methanol (2 mL) in accordance with the procedure described above. The yield was 82.4 mg (78%). Results of ^{1}HNMR (400MHz, $CDCl_3$) were as follows: δ 10.23 (s, 1H, meso-H); 9.75 (s, 1H, meso-H); 9.00 (s, 1H, meso-H); 5.98 (q, 1H, $CH_3\underline{CH}OMe$); 5.20 (m, 1H, 17-H); 4.68 (m, 1H, 18-H); 3.85 (q, 2H, $\underline{CH_2}CH_3$); 3.80 (s, ^{3}H, $CO_2\underline{Me}$); 3.70 (s, ^{3}H, $O\underline{Me}$); 3.60, 3.50 and 3.40 (each s, ^{3}H, ring-CH_3); 2.89 (m, 1H, $CH_2\underline{CH}CO_2Me$); 2.75 (m, 1H, $CH_2\underline{CH}CO2Me$); 2.42–2.30 (m, 2H, $\underline{CH_2}CH_2CO_2Me$); 2.21 (d, ^{3}H, $\underline{CH_3}CHOMe$); 1.95 (d, ^{3}H, 18-CH_3); 1.75 (t, ^{3}H, $CH_2\underline{CH_3}$); 0.12 (s, 1H, NH) and –2.40 (s, 1H, NH). The HRMS for $C_{35}H_{38}N_4O_5$ was calculated as 594.2842 and observed to be 595.2919(MH^+).

Methyl 3-(1′-pentyloxyethyl)-3-devinyl-13^2-oxopyropheophorbide-a (**8**): This title compound was prepared from pyrodione **3** (100.0 mg; 0.178 mmol) and an excess of pentyl alcohol (2 mL), as described above. The yield was 95.9 mg (83.0%). Results of ^{1}HNMR (400MHz, $CDCl_3$) were as follows: δ 10.39 (d, 1H, meso-H); 9.46 (d, 1H, meso-H); 9.08 (s, 1H, meso-H), 6.09 (q, 1H, $CH_3\underline{CH}OPentyl$); 5.22 (m, 1H, 17-H); 4.23 (m, 1H, 18-H); 3.75 (q, 2H, $\underline{CH_2}CH_3$); 3.70 (s, ^{3}H, $CO_2\underline{Me}$); 3.69 (t, 2H, O-$\underline{CH_2}CH_2$); 3.58, 3.45 and 3.40 (each s, ^{3}H, ring-CH_3); 2.90 (m, 1H, $CH_2\underline{CH}CO_2Me$); 2.75 (m, 1H, $CH_2\underline{CH}CO_2Me$); 2.45 (m, 2H, $\underline{CH_2}CH_2CO_2Me$); 2.25 (dd,

^{3}H, $\underline{CH_3}$CH-OPentyl); 1.96 (dd, ^{3}H, 18-CH_3); 1.85 (m, 2H, $OCH_2\underline{CH_2}$); 1.70 (t, ^{3}H, $CH_2\underline{CH_3}$-ring); 1.50–1.40 (m, 2H, CH_2-Pentyl); 1.42–1.25 (m, 2H, CH_2-Pntyl); 0.85 (t, ^{3}H, CH_3-Pentyl); 0.12 (s, 1H, NH); –2.40 (s, 1H, NH). The HRMS for $C_{39}H_{46}N_4O_5$ was calculated as 650.3468 and observed to be 651.3545(MH^+).

Methyl 3-(1′-heptyloxyethyl)-3-devinyl-13^2-oxopyropheophorbide-a (**9**): This compound was prepared from pyrodione **3** (100.0 mg; 0.178 mmol) and an excess of heptyl alcohol (2 mL), as described above. The yield was 86.83 mg (72.0%). Results of ^{1}HNMR (400MHz, $CDCl_3$) were as follows: δ 10.35 (d, 1H, meso-H); 9.62 (d, 1H, meso-H); 9.00 (s, 1H, meso-H); 6.01 (q, 1H, $CH_3\underline{CH}$-Oheptyl); 5.25 (m, 1H, 17-H); 4.72 (m, 1H, 18-H); 3.75 (q, 2H, $\underline{CH_2}CH_3$-ring); 3.70 (t, 2H, O-$\underline{CH_2}CH_2$); 3.65 (s, ^{3}H, $CO_2\underline{Me}$); 3.63, 3.55 and 3.40 (each s, ^{3}H, ring-CH_3); 2.85 (m, 1H, $CH_2\underline{CH}CO_2Me$); 2.70 (m, 1H, $CH_2\underline{CH}CO_2Me$); 2.38 (m, 2H, $\underline{CH_2}CH_2CO_2Me$); 2.25 (d, ^{3}H, $\underline{CH_3}$CH-Oheptyl); 1.97 (s, ^{3}H, 18-CH_3); 1.85 (m, 2H, $OCH_2\underline{CH_2}$); 1.75 (t, ^{3}H, $CH_2\underline{CH_3}$-ring); 1.51–1.38 (m, 2H, CH_2-heptyl); 1.30–1.15 (m, 6H, 3CH_2-hetyl); 0.78 (t, ^{3}H, CH_3-heptyl); 0.20 (brs, 1H, NH) and –2.08 (brs, 1H, NH). The HRMS for $C_{41}H_{50}N_4O_5$ was calculated and observed to be 679.3857(MH^+).

Methyl 3-(1′-decyloxyethyl)-3-devinyl-13^2-oxopyropheophorbide-a (**10**): The product was prepared from pyrodione **3** (100.0 mg; 0.178 mmol) and an excess of decyl alcohol (2 mL), as described above. The yield was 96.0 mg (75.0%). Results of ^{1}HNMR (400MHz, $CDCl_3$) were as follows: δ 10.35 (d, 1H, meso-H); 9.55 (d, 1H, meso-H); 9.02 (s, 1H, meso-H); 6.05 (q, 1H, $CH_3\underline{CH}$-Odecyl); 5.25 (m, 1H, 17-H); 4.72 (m, 1H, 18-H); 3.78 (q, 2H, $\underline{CH_2}CH_3$-ring); 3.70 (t, 2H, O-$\underline{CH_2}CH_2$); 3.55 (s, ^{3}H, $CO_2\underline{Me}$); 3.53, 3.51 and 3.40 (each s, ^{3}H, ring-CH_3); 2.85 (m, 1H, $CH_2\underline{CH}CO_2Me$); 2.75 (m, 1H, $CH_2\underline{CH}CO_2Me$); 2.42–2.30 (m, 2H, $\underline{CH_2}CH_2CO_2Me$); 2.30 (d, ^{3}H, $\underline{CH_3}$CH-Odecyl); 1.93 (s, ^{3}H, 18-CH_3); 1.82 (m, 2H, $OCH_2\underline{CH_2}$-decyl); 1.72 (t, ^{3}H, $CH_2\underline{CH_3}$-ring); 1.50–1.40 (m, 2H, CH_2-decyl); 1.41–1.20 (m, 12H, 6CH_2-decyl); 0.80 (t, ^{3}H, CH_3-decyl); 0.20 (brs, 1H, NH) and –2.09 (brs, 1H, NH). The HRMS for $C_{44}H_{56}N_4O_5$ was calculated as 720.4251 and observed to be 721.4322(MH^+).

Cu(II) complex of methyl 13^2-oxopyropheophorbide-a (**5**): Pyrodione **3** (50.0 mg; 0.089 mmol) was dissolved in chloroform (10 mL) and placed in a 100 mL reaction flask. Cupric acetate (1.0 g) that had been dissolved in methanol (40 mL) was then added. The reaction mixture was stirred under nitrogen atmosphere at room temperature for 2 h. It was washed with water and the organic layer was separated, dried over sodium sulfate and concentrated. The crude residue was purified by silica column chromatography by use of 5% methanol-dichloromethane as the eluant. Evaporation of the eluant produced a green solid. The yield was 21.0 mg (39%). The HRMS for $C_{34}H_{32}CuN_4O_4$ was calculated as 623.1820 and observed to be 624.2011(MH^+). The UV-Vis λ_{max}(CH_2Cl_2) was 423 nm (ε 43 350), 524 (ε 4800) and 659 (ε 33 330).

Zn(II) complex of methyl 13^2-oxopyropheophorbide-a (**6**): Pyrodione **3** (50.0 mg; 0.089 mmol) was dissolved in dichloromethane (10 mL) and placed in a 100 mL reaction flask. Zinc acetate (500.0 mg) that had been dissolved in methanol (40 mL) was added. The mixture was stirred under nitrogen at room temperature for 2 h. It was then washed with water and the organic layer was separated, dried over sodium sulfate and concentrated. The product, a green solid, was obtained by means of the method described above for the copper complex. The yield was 46.0 mg (84%). UV-Vis λ_{max}(CH_2Cl_2) was 423 nm (ε 68 550), 534 (ε 5350) and 662 (ε 49 000). Results of ^{1}HNMR (400 MHz, $CDCl_3$) were as follows: δ 9.35 (s, 1H, meso-H); 9.19 (s, 1H, meso-H); 8.45 (s, 1H, meso-H); 7.95(dd, 1H, $\underline{CH}$=CH_2); 6.24–6.20 (dd, 2H, CH=$\underline{CH_2}$); 4.90 (m, 1H, 17-H); 4.81–4.75 (m, 1H, 18-H); 3.80 (q, 2H, $\underline{CH_2}CH_3$); 3.75 (s, ^{3}H, $CO_2\underline{Me}$); 3.65, 3.45 and 3.40 (each s, ^{3}H, ring-CH_3); 3.00 (m, 1H, $CH_2\underline{CH}CO_2Me$); 2.95 (m, 1H, $CH_2\underline{CH}CO_2Me$); 2.65 (m, 1H, $\underline{CH}CH_2CO_2Me$); 2.51 (m, 2H, $\underline{CH}CH_2CO_2Me$) and 1.85–1.70 (m, 6H, $CH_2\underline{CH_3}$, 18-CH_3). The HRMS for $C_{34}H_{32}N_4O_4Zn$ was calculated as 624.1715 and observed to be 625.1912(MH^+).

General procedure for synthesis of indium(III) complexes. In a 100 mL reaction flask, alkyl ether derivatives **7–10** (50.0 mg) individually were dissolved in 15 mL benzene, and sodium acetate (500.0 mg), anhydrous K_2CO_3 (500.0 mg) and indium(III) chloride (300.0 mg) were added. The reaction mixture was refluxed under nitrogen overnight (for approximately 15 h). The reaction was monitored to completion by UV-vis spectroscopy. The mixture was neutralized with acetic acid, and washed with water (3 × 100 mL). The organic layer was separated and dried over sodium sulfate. The solvents were then removed under high vacuum at room temperature. The purified products were obtained as green solids after silica column chromatography with 5–10% methanol-dichloromethane as eluting solvents.

In(III) complex of methyl 13-oxo-pyropheophorbide-a (**4**): This title compound was prepared from pyrodione **3** (50. 0 mg) and indium(III) chloride (300.0 mg) by means of the general procedure for the synthesis of indium complexes (described above). The yield was 22.0 mg (35.0%) as a mixture of two isomers. The UV-Vis λ_{max}(CH_2Cl_2) was 423 nm (ε 96, 570) and 664 (ε 57 100). The results of ^{1}HNMR (400 MHz, $CDCl_3$) were as follows: δ 10.02 (two sets of signals, 1H, meso-H); 9.83 (two sets of signals, 1H, meso-H); 8.95 (two sets of signals, 1H, meso-H); 8.00 (dd, 1H, $\underline{CH}$=CH_2); 6.24–6.20 (ddd, 2H, CH=$\underline{CH_2}$); 5.19 (m, 1H, 17-H); 4.81–4.75 (m, 1H, 18-H); 3.90 (q, 2H, $\underline{CH_2}CH_3$); 3.85 (s, ^{3}H, $CO_2\underline{Me}$); 3.65, 3.45 and 3.40 (each s, ^{3}H, ring-CH_3); 2.95 (m, 1H, $CH_2\underline{CH}CO_2Me$); 2.75 (m, 1H, $CH_2\underline{CH}CO_2Me$); 2.60 (m, 1H, $\underline{CH}CH_2CO_2Me$); 2.49 (m, 2H, $\underline{CH}CH_2CO_2Me$) and 1.85–1.70 (m, 6H, $CH_2\underline{CH_3}$, 18-CH_3). The title compound, obtained as an isomeric mixture, was separated into individual isomers. The HRMS for $C_{34}H_{32}ClInN_4O_4$ (mixture) was calculated as 710.1151 and observed to be 711.1227(MH^+). With regard to the individual isomers, the faster moving band (**A**) was observed to be 710.1158 and the slower moving band (**B**) was observed to be 710.1152.

In(III) complex of methyl 3-(1′-methyloxyethyl)-3-devinyl-13^2-oxopyropheophorbide-a (**11**): This product was prepared from pyrodione-methyl ether **7** (50.0 mg) and indium(III) chloride (300.0 mg), as described above. The yield was 17.4 mg (28.0%). Results of ^{1}HNMR (400MHz, $CDCl_3$, isomeric mixture) were as follows: 10.10–10.00 (two sets of signals, 1H, meso-H); 9.62–9.58 (two sets of signals, 1H, meso-H); 8.92 (two sets of signals, 1H, meso-H); 5.80–5.70 (m, 1H, $CH_3\underline{CH}$OMe); 5.20 (m, 1H, 17-H); 4.81–4.75 (m, 1H, 18-H); 3.85–3.83 (m, 5H, $\underline{CH_2}CH_3$ ring, $CO_2\underline{Me}$); 3.75 (s, ^{3}H, O$\underline{Me}$); 3.29, 3.27 and 3.10 (each s, ^{3}H, ring-CH_3); 2.93 (m, 1H, $CH_2\underline{CH}CO_2Me$); 2.73 (m, 1H, $CH_2\underline{CH}$CO2Me); 2.61 (m, 2H, $\underline{CH}CH_2CO_2Me$); 2.48 (m, 1H, $\underline{CH}CH_2CO_2Me$); 2.10 (d, ^{3}H, $\underline{CH_3}$CHOMe) and 1.80–1.70 (m, 6H, 18-CH_3, $CH_2\underline{CH_3}$). The HRMS for $C_{35}H_{36}ClInN_4O_5$ was calculated as 742.1413 and observed to be 708.1802(MH^+-Cl).

In(III) complex of methyl 3-(1′-pentyloxyethyl)-3-devinyl-13^2-oxopyropheophorbide-a (**12**): This compound was prepared from pyrodione-pentyl ether **8** (50.0 mg) and indium(III) chloride (300.0 mg), as described above. The yield was 14.1 mg (25.0%). Results of ^{1}HNMR (400Mhz, $CDCl_3$, isomeric mixture) were as follows: 10.05 (two sets of signals, 1H, meso-H); 9.70 (two sets of signals, 1H, meso-H); 9.00 (two sets of signals, 1H, meso-H); 5.88 (m, 1H, $CH_3\underline{CH}$Opentyl); 5.22 (m, 1H, 17-H); 4.80(m, 1H, 18-H); 3.90 (m, 5H, $\underline{CH_2}CH_3$-ring, $CO_2\underline{Me}$); 3.70 (t, 2H, O-$\underline{CH_2}$-pentyl); 3.45, 3.30 and 3.28 (each s, ^{3}H, ring-CH_3); 3.10–2.90 (m, 1H, $CH_2\underline{CH}CO_2Me$); 2.85–2.80 (m, 1H, $CH_2\underline{CH}CO_2Me$); 2.79–2.70 (m, 1H, $\underline{CH}CH_2CO_2Me$); 2.68–2.60 (m, 1H, $\underline{CH}CH_2CO_2Me$); 2.40 (dd, ^{3}H, $\underline{CH_3}$CH-OPentyl); 2.10 (m, ^{3}H, 18-CH_3); 1.85–1.70 (m, 6H, $CH_2\underline{CH_3}$-ring & 2$\underline{CH_2}$-pentyl); 1.40–1.30 (m, 2H, CH_2-Pentyl) and 0.90 (m, ^{3}H, CH_3-pentyl). The HRMS for $C_{39}H_{44}ClInN_4O_5$ was calculated as 798.2039 and observed to be 799.2111(MH^+).

In(III) complex of methyl 3-(1′-heptyloxyethyl)-3-devinyl-13^2-oxopyropheophorbide-a (**13**): This title compound was obtained by reacting pyrodione-heptyl ether **9** (50.0 mg) with indium(III) chloride (300.0 mg), using the procedure described above. The yield was 17.0 mg (28.0%). Results of ^{1}HNMR (400MHz, $CDCl_3$) were as follows: δ 9.95 (two sets of signals, 1H, meso-H); 9.61–9.50 (two sets of signals, 1H, meso-H); 8.90–8.80 (two sets of signals, 1H, meso-H); 5.70–5.65 (m, 1H, $CH_3\underline{CH}$-Oheptyl); 5.16 (m, 1H, 17-H); 4.75–4.63 (m, 1H, 18-H); 3.81 (m, 5H, $\underline{CH_2}CH_3$-ring, $CO_2\underline{Me}$); 3.65 (m, 2H, O-$\underline{CH_2}CH_2$); 3.58 (m, ^{3}H, ring-CH_3); 3.30 (m, ^{3}H, ring-CH_3); 3.25 (m, ^{3}H, ring-CH_3); 2.95 (m, 1H, $CH_2\underline{CH}CO_2Me$); 2.85 (m, 1H, $CH_2\underline{CH}CO_2Me$); 2.65–2.55 (m, 2H, $\underline{CH_2}CH_2CO_2Me$); 2.35 (m, ^{3}H, $\underline{CH_3}$CH-Oheptyl); 2.05 (m, ^{3}H, 18-CH_3); 1.80–1.70 (m, 5H, $OCH_2\underline{CH_2}$, $CH_2\underline{CH_3}$-ring); 1.60–1.50 (m, 4H, 2CH_2-heptyl); 1.30–1.20 (m, 4H, 2CH_2-heptyl) and 0.85 (m, ^{3}H, CH_3-heptyl). The HRMS for $C_{41}H_{48}ClInN_4O_5$ was calculated as 826.2352 and observed to be 827.2428(MH^+).

In(III) complex of methyl 3-(1′-decyloxyethyl)-3-devinyl-13^2-oxopyropheophorbide-a (**14**): This was prepared from pyrodione-decy ether **10** (50.0 mg) and indium(III) chloride (300.0 mg), as described above. The yield was 19.2 mg (32.0%). Results of ^{1}HNMR (400 MHz, $CDCl_3$) were as follows: 10.00 (two sets of signals, 1H, meso-H); 9.60–9.50 (two sets of signals, 1H, meso-H); 8.95–8.80 (two sets of signals, 1H, meso-H); 5.78–5.72 (m, 1H, $CH_3\underline{CH}$-Odecyl); 5.18 (m, 1H, 17-H); 4.75 (m, 1H, 18-H); 3.91–3.80 (m, 5H, $\underline{CH_2}CH_3$-ring, $CO_2\underline{Me}$); 3.65 (m, 2H, O-$\underline{CH_2}CH_2$); 3.50, 3.41 and 3.25 (each s, ^{3}H, ring-CH_3); 2.95 (m, 1H, $CH_2\underline{CH}CO_2Me$); 2.79 (m, 1H, $CH_2\underline{CH}CO_2Me$); 2.60–2.50 (m, 2H, $\underline{CH_2}CH_2CO_2Me$); 2.40–230 (m, 4H, 2$\underline{CH_2}$-decyl); 2.20 (d, ^{3}H, $\underline{CH_3}$CH-Odecyl); 2.00 (m, ^{3}H, 18-CH_3); 1.81–1.65 (m, 7H, $CH_2\underline{CH_3}$-ring, 2$\underline{CH_2}$-decyl); 1.40–1.10 (m, 8H, 4CH_2-

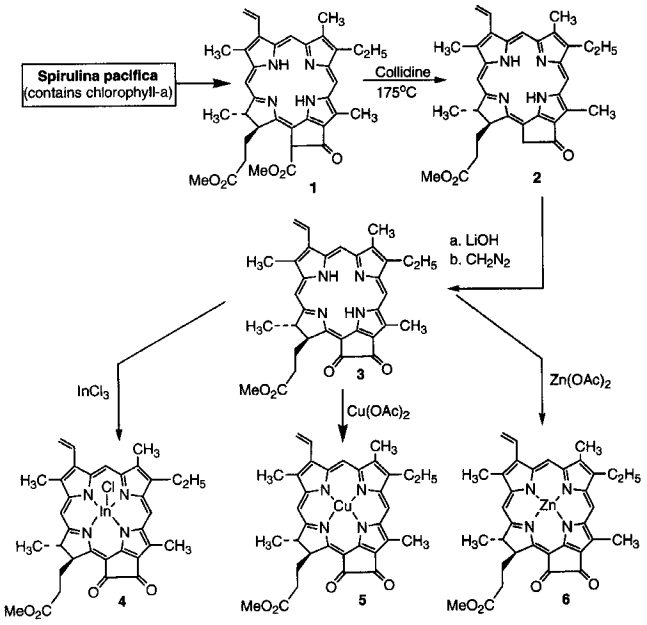

Scheme 1.

decyl) and 0.90–0.80 (m, ^{3}H, CH_3-decyl). The HRMS for $C_{44}H_{54}ClInN_4O_5$ was calculated as 868.2822 and observed to be 869.2886(MH^+).

The extinction coefficient values of the alkyl ether analogs (**7–10**) and the corresponding In(III) complexes (**12–14**) were as follows: for the free-base analogs the UV-Vis $\lambda_{max}(CH_2Cl_2)$ was 386 nm (ε 96 300), 512 (ε 11 200) and 670 (ε 57 300); and for the In(III) derivatives the UV-Vis $\lambda_{max}(CH_2Cl_2)$ was 422 nm (ε 96 900), 529 (ε 7280) and 655 (ε 60 000).

Instrumentation and methods for photophysical studies. Steady state measurements at room temperature were performed using a Shimadzu UV-3101PC spectrophotometer (for absorption spectra) and a Fluorolog-3 spectrofluorometer (Jobin Yvon) (for fluorescence spectra).

A SPEX 270M spectrometer (Jobin Yvon) equipped with an InGaAs photodetector (Electro-Optical Systems Inc.) was used for acquisition of the singlet oxygen emission spectra in organic solvents. A PMT module H9170-75 (Hamamatsu), attached to the SPEX 270M spectrometer, was used to obtain singlet oxygen phosphorescence spectra from Tween-80/water suspensions of the studied compounds. A diode-pumped solid-state laser (Verdi, Coherent) at 532 nm was used as the excitation source. The sample solution in a quartz cuvette was placed directly in front of the entrance slit of the spectrometer and the exciting laser beam was directed at 90° relative to the collection of emission. Longpass filters (538AELP and 950 LP; Omega Optical) were used to attenuate the scattered excitation light and fluorescence from the samples.

Sample solutions in organic solvents (chloroform, toluene and methanol) were prepared by mixing a small amount of the chloroform stock solution (5 mg/mL) with solvent. Rhodamine 6G and Rose Bengal were used as references for measuring the fluorescence and singlet oxygen yields. During the measurements, the optical densities of the sample solutions were equalized at the excitation wavelength (532 nm). The fluorescence quantum yield (Φ_{Fl}) for Rhodamine 6G in methanol is 0.93 (33) and the singlet oxygen yield (Φ_{Δ}) for Rose Bengal in methanol is 0.80 (34). Singlet oxygen yield was first determined for the In(III) complex in methanol, which was then used as a reference when comparing the free-base complex and the In(III) complex in different solvents.

Formulation of photosensitizers. In a typical procedure the photosensitizer (3 mg) was mixed with Tween 80 (0.1 mL) on a marble mortar and incubated for 24 h at ambient temperature with occasional grinding; D5W (10 mL) was then slowly added with continuous mixing. The solution was then passed through a 0.22 μm filter and the concentration of the filtrate was determined spectrophotometrically (Beer Lambert's equation) (35).

In vitro *photosensitizing efficacy.* The photosensitizing activity was determined in the RIF tumor cell line using the colorimetric MTT assay (36). The RIF tumor cells were maintained in complete medium that consisted of α-MEM with 10% fetal calf serum, L-glutamine, penicillin and streptomycin at 37°C, 5% CO_2, 95% air and 100% humidity. Cells were seeded in 96-well plates at a density of 5×10^3 cells/well in complete medium. After overnight incubation at 37°C the photosensitizers were added at variable concentrations up to 1 μ*M* and incubated at 37°C for 24 h in the dark. Before light treatment the medium was replaced with drug-free complete medium. Cells were then illuminated (0–4 J/cm^2) with 665 nm light from an argon-pumped dye laser at a fluence rate of 3.2 mW/cm^2. After PDT the cells were incubated for 48 h at 37°C in the dark. During the last 4 h of incubation, 10 μL of a 4.0 mg/mL solution in PBS of 3-[4,5-dimethylthiazol-2-yl]-2,5-diphenyltetrazoliumbromide (MTT) (Sigma, St. Louis, MO) was added to each well. After 4 h the MTT and medium were removed and 100 μL DMSO was added to solubilize the formazan crystals. Absorbances were read on a microtiter plate reader (Titertek Multiscan Plus MK II; Miles Inc.) at 560 nm. The results were plotted as the survival rate of treated cells versus untreated control cells (*i.e.* those exposed to no drug and no light) for each compound tested. Each data point represents the mean value from 3 separate experiments and the SEMs were <10%. Each experiment was done with 5 replicate wells.

In Vivo *photosensitizing efficacy.* The *in vivo* efficacy of these compounds was determined in C3H/HeJ mice that received subcutaneously transplanted RIF tumors. Each compound was initially evaluated at three different doses (0.25, 0.5 and 1 μmol/kg) in groups of three mice/dose. The tumors were treated when they reached a diameter of 4–5 mm. The photosensitizers were injected in the tail vein and the tumor was irradiated (135 J/cm^2 at 75 mw/cm^2) 24 h after injection. The tumor regrowth was monitored until it reached 400 mm^3 or for 30 days. Once the optimal drug dose was determined, each photosensitizer was further evaluated using twelve mice per group.

Intracellular localization. RIF cells were grown on poly-l-lysine–coated coverslips in six-well plates. Photosensitizers at 1 μ*M* were added in growth medium and incubated for 24 h. Organelle-specific fluorescent probes (Molecular Probes) were coincubated with the photosensitizers before examination by fluorescence microscopy. The following probes were used: for mitochondria, Mitotracker green (MTG) (37), 1 μ*M* for 1 h before examination; for lysosomes, Fluospheres 505/515 yellow green 0.1 μm in diameter (1:10 000 dilution) for 24 h with gentle rocking (28); for Golgi apparatus, Bodipy FL C5 Ceramide (38) in the form of bovine serum albumin (BSA) complexes, 5 μ*M* as indicated by the manufacturer's protocol. Cells were examined by fluorescence microscopy (Zeiss Axiovert 200 Inverted microscope) with a Fluoarc mercury vapor shortarc lamp as the light source. Images were collected with the AxioCam MR-MRGrab Frame grabber and processed with AxioVision LE 4.1 imaging software. The individual fluorochromes were examined with the following filter combinations from ChromaTechnology: for the photosensitizers, Ex BP D410/40, BeamSplitter FT 505dcxvu, Em BP 675/50; for MTG and Fluospheres, Set 38 1031-346, Ex BP 470/40, BeamSplitter FT 495, Em BP 525/50; for Bodipy C5 Ceramide, Set 31 1031-350, Ex BP 565/30, BeamSplitter FT 585, Em BP 520/60.

RESULTS AND DISCUSSION

Chemistry

We have previously shown that pyropheophorbide-a **2** can be converted into the corresponding enolate in a reaction with aqueous LiOH-THF, which, during *in situ* oxidation, resulted in a 75% yield of the corresponding 13^2-oxo derivative **3** (39). We used this methodology for the preparation of pyrodione **3**, which was used as a substrate for further substitutions. In tetrapyrrolic systems, certain metal complexes, such as Zn(II), Cu(II), Sn(II) and In(III), were generally found to have a significant impact on the photosensitizing efficacy of various porphyrin systems (40). In most of the free-base and metalated photosensitizers (except for the Cu(II) complex of benzochlorin) changes in the formation of singlet oxygen when the photosensitizer in the tumor is exposed to light are believed to be one of the main causes of cytotoxicity. To investigate the effect of these metals on the photochemical activity of pyrodione **3**, it was converted into the corresponding In(III), Cu(II) and Zn(II) complexes **4**, **5** and **6** respectively (Scheme 1).

It is now well established that the lipophilicity of a molecule can play a significant role in its *in vivo* photosensitizing efficacy and

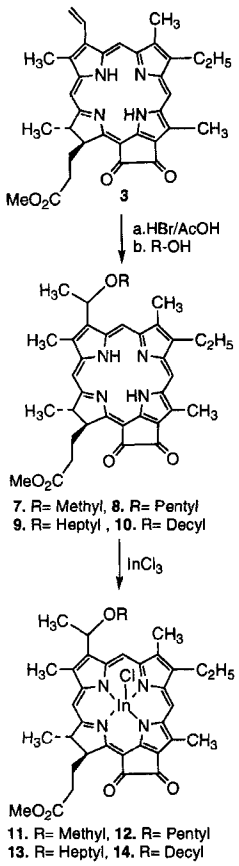

Scheme 2.

can easily be altered by introducing alkyl chains that have various numbers of carbons. In pyropheophorbide-a, purpurinimide and bacteriopurpurinimide systems (4), among the alkyl ether analogs, photosensitizers containing alkyl ether functionalities at position-3 were found to be more effective than photosensitizers with alkyl ether functionalities at other peripheral positions (*i.e.* 8, 12 or 20). Therefore, in the present study pyrodione **3** was converted into a series of 3-substituted alkyl ether analogs (methyl **7**, pentyl **8**, heptyl **9** and decyl **10**), on the basis of the reaction sequences in Scheme 2. In addition, among the metal complexes, because the In(III) pyrodione **4** was the most effective, the 3-substituted alkyl ether analogs **7–10** were converted into the corresponding In(III) complexes **11–14** (Scheme 2).

Photophysical studies: effect of In(III) as a central metal

The absorption spectra of the free-base (**10**) and the In(III) complex (**14**) of the decyl ether analog of methyl 13-oxopyropheophorbide-a in chloroform and methanol are shown in Fig. 2. Complexing with indium leads to a blue spectral shift (~13 nm) in the peak position of the long-wavelength Q band (665 nm *versus* 678 nm). Similar hypsochromic shifts are well-known for metal complexes of porphyrin-type molecules (41–44) and can be considered as a measure of the degree of interaction of the metal ion and the porphyrin π-electron system (42). It is supposed to be caused by the distortion of the ligand plane with incorporation of the central ion (43,44). There are also changes in the position and shape of the Soret band of **10**, compared with **14** in MeOH (Fig. 2:4) chloroform (Fig. 2:2) and toluene (data not shown).

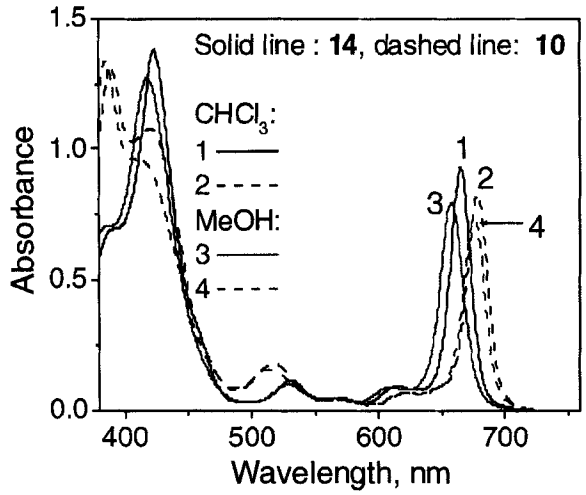

Figure 2. Absorption spectra of **14** and **10** in chloroform (1, 2) and methanol (3, 4).

Fluorescence spectra of **10** and **14** in chloroform, toluene and methanol are shown in Fig. 3. The difference between the intensities of fluorescence of **10** and **14** solutions in chloroform (and toluene) is quite striking. The fluorescence quantum yield for **10** in $CHCl_3$ is low ($\Phi_{Fl\ 10} \approx 0.06$), but a further decrease to one tenth of this was observed for the corresponding In(III) metal complex (Fig. 3). The heavy atom effect of an atom coordinated with a porphyrin-type ligand (41–45) should be accompanied by an increase in intersystem crossing and triplet yield (42,43,45), which correlates with singlet oxygen yield. However, **10** and **14** unexpectedly showed similar results in $CHCl_3$ and toluene for the production of singlet oxygen. For compound **10** the singlet oxygen yield Φ_Δ was 85–88% of that of **14** (Fig. 4A). The singlet oxygen yield for **14** was determined in methanol to be 0.72, using the Rose Bengal methanol solution as a reference. Correspondingly, for **10**, the singlet oxygen yield is 0.61–0.63. These values are close to those reported for the structurally related purpurins and chlorins (46). The absence of a stronger effect on singlet oxygen generation produced by incorporation of In(III) into the pyrodione can be explained by that fact that, as the rate of $S_1 \rightarrow T_1$ intersystem crossing increases, the heavy atom simultaneously increases the rate of $T_1 \rightarrow S_0$ nonradiative transition (42,43), resulting in a decrease in the triplet lifetime and, correspondingly, in the efficiency of the sensitization of singlet oxygen (43,45). However, for the solutions of **10** and **14** in methanol, a difference in singlet oxygen production is larger; the singlet oxygen yield for **10** in methanol is quite low (Fig. 4B). The low Φ_Δ for **10** could be associated with its aggregation in MeOH. In fact, the fluorescence of **10** is significantly quenched (a signature of aggregation) in MeOH, compared with $CHCl_3$ and toluene as solvents (Figs. 3, 2, 4 and 6). The change in the shape of the Soret band for **10** in the different solvents reported above also is indicative of aggregation.

Zenkevich *et al.* (46) reported similar differences in the fluorescence and singlet oxygen yields for purpurins and chlorins structurally related to **10** in different solvents. However, they concluded that the singlet oxygen quantum yield for purpurins and chlorins does not appear to depend noticeably on medium polarity and that a decrease in Φ_{Fl} and Φ_Δ in some cases is due to the low solubility of the compounds and the aggregation effects caused by stacking of the planar molecules (46). The efficiency of singlet

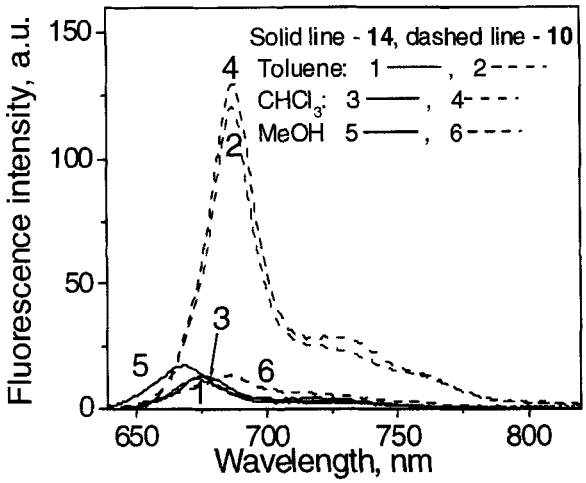

Figure 3. Fluorescence spectra of **14** and **10** in toluene (1, 2), chloroform (3, 4) and methanol (5, 6). OD was equalized at the excitation wavelength (532 nm).

oxygen generation and the *in vitro* and *in vivo* photodynamic efficacy of such low solubility compounds may therefore depend significantly on the formulation for administration, and its subsequent distribution *in vitro* and *in vivo*. Irradiation of a suspension of **10** in Tween-80/H_2O produces approximately 50% of the singlet oxygen yield shown by **14** in Tween-80/H_2O (Fig. 4C). This is considerably better than in MeOH but not as good as in toluene or $CHCl_3$. It means that the molecules of **10** in Tween-80/H_2O are still aggregated to some extent. The situation for the In(III) complex seems to be different. The existence of a complexed metal ion does not necessarily hinder aggregation (47). Metalloporhyrins remain planar, which is favorable to the formation of stacked aggregates. If the ionic radius of the metal is too large to fit into the center of the macrocycle, the metal ion is located outside of the ligand plane and distorts the porphyrin system (44). This creates a steric hindrance that interferes with the stacking of porhyrin-type molecules into aggregates. In the case of **14**, in addition to the In(III) ion, there also is a chlorine atom located outside of the ligand plane, which could certainly hamper aggregation.

In Vitro photosensitizing activity

Methyl 13^2-oxopyropheophorbide-a and the related compounds, **3-14**, were evaluated by MTT assay for *in vitro* photosensitizing efficacy at different light doses and drug concentrations (36) (Fig. 5).

As can be seen, among the metalated complexes, only the In(III) complex **4** showed enhanced activity, compared with the starting material **3** (Fig. 5A) and both the possible isomers of **4** were found to be equally effective (Fig. 5B). As expected, the related Cu(II) derivative **5** with no singlet oxygen–producing capability did not show any *in vitro* photoactivity, thereby indicating the importance of singlet oxygen in photodynamic therapy with this series of compounds. Among the alkyl ether derivatives both the free-base **7–10** and the corresponding In(III) complexes **11–14** showed a correlation between lipophilicity and photosensitizing efficacy. For example in both series, the most lipophilic decyl ether derivatives (containing 10 carbon units) were the most effective (Fig. 5C,D). The In(III) complexes were generally found to be more effective than the corresponding free-base analogs. For example, after irradiation of cells with 0.25 J/cm^2 light, 1 μM of the decyl

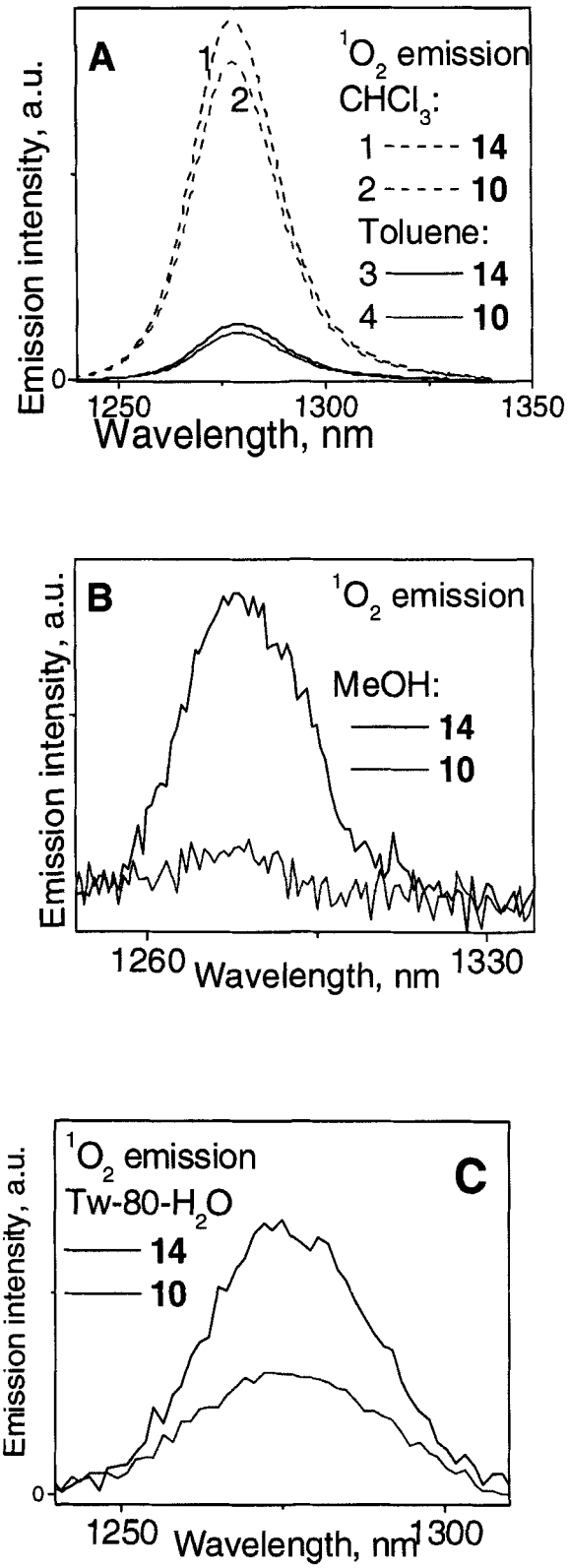

Figure 4. Phosphorescence of singlet oxygen sensitized by **14** and **10** in toluene and chloroform (A), MeOH (B) and Tween-80/H20 (C). OD was equalized at the excitation wavelength (532 nm).

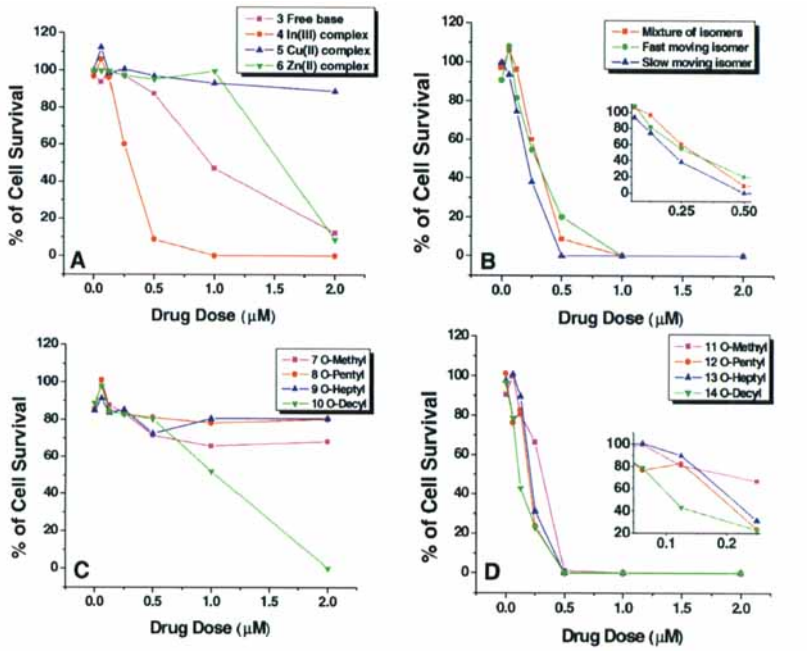

Figure 5. *In vitro* photosensitizing activity of compounds in RIF cells at different concentrations and a light dose of 0.25 J/cm^2. A: Free-base **3** and its metal complexes; B: isomers of the indium complex of pyrodione **4**; C: alkyl ether analogs of pyrodione **7–10**; and D: the corresponding In(III) complexes **11–14**.

ether analog **10** was required to kill 50% of the cells, whereas only 0.35 μ*M* of the corresponding In(III) complex **14** was required to achieve a similar result (Fig. 5D).

In Vivo photosensitizing activity

The free-base decyl ether analog of methyl 13-oxopyropheophorbide-a **10** and the corresponding In(III) complex **14** were the most effective *in vitro* photosensitizers. Therefore, these compounds were selected for a comparative *in vivo* efficacy analysis in mice with RIF tumors. The initial screening was performed with different drug doses, keeping other variables (*i.e.* light fluence and fluence rate [135 J/cm^2/75 mW/cm^2]) constant. Under these conditions, the In(III) complex **14** was more effective than **10**. As can be seen in Fig. 6, at both 0.25 and 0.50 μmol/kg compound **10** did not show any significant photosensitizing efficacy and only a slight delay in tumor growth was observed at higher doses. In contrast, compound **14** produced a significant delay in tumor growth at a dose of 0.25 μmol/kg, whereas a dose of 0.50 μmol/kg resulted in a 42% cure rate (*i.e.* 5/12 mice were tumor free on day 30).

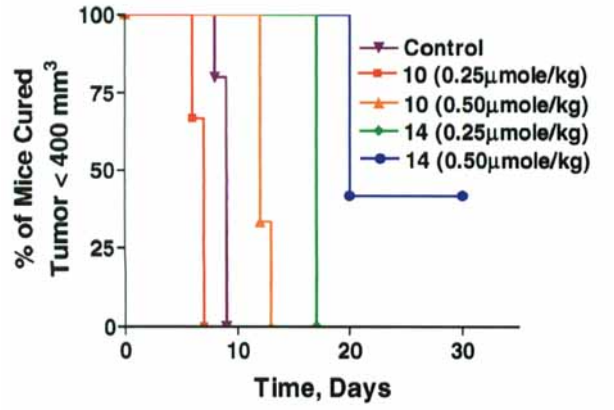

Figure 6. Comparative *in vivo* photosensitizing efficacy of the decyl-ether derivative **10** and the corresponding In(III) complex **14** in C3H mice (12 mice/group) bearing RIF tumors. The tumors were exposed to light (135 J/cm^2; 75 mW/cm^2) 24 h after injection of the photosensitizer.

Intracellular localization

No colocalization was observed between MTG or Fluospheres and the photosensitizers (data not shown). The compounds containing the di-keto functionalities were colocalized with Bodipy C5 ceramide (a probe for Golgi apparatus). No shift in localization was observed upon insertion of the In(III) into the macrocycle. Figure 7 shows fluorescence images of cells incubated with Bodipy C5 ceramide (green) alongside those with compounds **10** and **14**

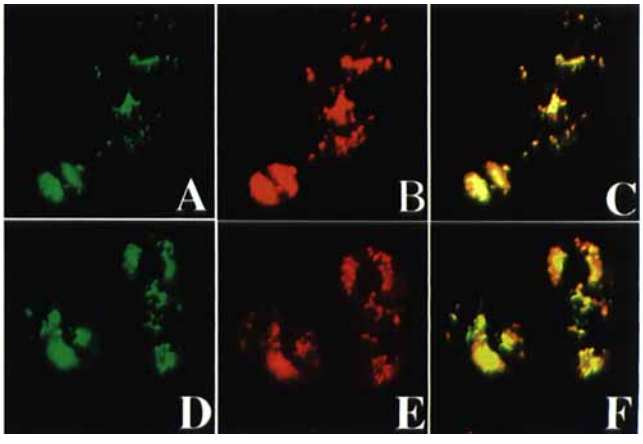

Figure 7. Subcellular localization of compounds 10 (top) and 14 (bottom) in RIF cells. Fluorescence images of the same fields. A, D: Bodipy C5 ceramide (Golgi-specific probe); B, E: photosensitizers 10 and 14, respectively; C, F: overlay of A and B, and D and E, respectively, demonstrating colocalization of the photosensitizers and the Golgi-specific probe.

(red). The overlay demonstrates the almost exclusive colocalization (yellow) in the Golgi apparatus.

CONCLUSIONS

In summary, the addition of an extra keto group to the five-membered exocyclic ring of pyropheophorbide-a causes a red shift in the absorption wavelength of the photosensitizer, permitting greater treatment depth. However, compared with the hexylether derivative of pyropheophorbide-a (HPPH), the structural change in the exocyclic ring of pyropheophorbide-a also diminishes its photosensitizing efficacy *in vitro* and *in vivo*. The decreased phototoxic effect may be due to a combination of diminished solubility, lower tumor uptake, more aggregation and decreased singlet oxygen production, combined with a shift in subcellular localization from mitochondria to the Golgi bodies, which may be less sensitive sites. Increasing the length of the alkyl ether chain appears to enhance the PDT effect. It was observed that insertion of In(III) into the macrocycle enhances the phototoxicity, although not to the extent found after chelation of In(III) to HPPH. In fact, *in vivo* the decreased effect on tumor response by introducing a second keto group into pyropheophorbide-a is restored by chelation of In(III). Chelation of In(III) does not change the site of localization and therefore enhances phototoxicity by another mechanism(s). Further mechanistic studies with these analogs are currently in progress.

Acknowledgements—We thank the National Institutes of Health (NIH; CA 55791), the Oncologic Foundation of Buffalo, the Roswell Park Alliance Foundation and the shared resources of the RPCI support grant (P30CA16056) for the financial assistance. The work performed at the Institute for Lasers, Photonics and Biophotonics (SUNY, Buffalo) was supported by the NIH (1R01CA104492-01A).

REFERENCES

1. Dougherty, T. J., C. Gomer, B. W. Henderson, G. Jori, D. Kessel, M. Korbelik, J. Moan and Q. Peng (1998) Photodynamic therapy. *J. Natl. Cancer Inst.* **90**, 889–905.
2. Olenick, N. L., R. L. Morris and I. Benchenko (2001) The role of apoptosis in response to photodynamic therapy: what, where, why and how? *Photochem. Photobiol. Sci.* **1**, 1–21.
3. Sherman, W. M., C. M. Allen and J. E. van Lier (2000) Role of activated oxygen species in photodynamic therapy. *Methods Enzymol.* **319**, 376–400.
4. Pandey R. K. and G. Zheng (2000) Porphyrins as photosensitizers in photodynamic therapy. In *The Porphyrin Handbook* (Edited by K. M. Smith, K. Kadish and R. Guilard), pp. 157–230. Academic Press, San Diego.
5. Ali, H and J. E. van Lier (1999) Metal complexes as a photo- and radiosensitizers. *Chem. Rev.* **99**, 2379–2450.
6. Wilson, B. C., M. S. Patterson and L. Lilge (1997) Implicit and explicit dosimetry in photodynamic therapy: a new paradigm. *Laser Med. Sci.* **12**, 182–199.
7. Lobel, J., I. J. MacDonald, M. J. Ciesielski, T. Barone, W. R. Potter, J. Pollina, R. J. Plunkett, R. A. Fenstermaker and T. J. Dougherty (2001) 2-[1-hexyloxyethyl]-2-devinylpyropheophorbide-a (HPPH) in a nude rat glioma model: implications for photodynamic therapy. *Laser Surg. Med.* **29**, 397–405.
8. Pandey, R. K., A. B. Sumlin, W. R. Potter, D. A. Bellnier, B. W. Henderson, S. Constantine, M. Aoudia, M. A. J. Rodgers, K. M. Smith and T. J. Dougherty (1996) Structure and photodynamic efficacy among alkyl ether analogs of chlorophyll-a. *Photochem. Phoobiol.* **63**, 194–205.
9. Morgan, A. R., D. Skalkos, G. Maguire, A. Rampersaud, G. Garbo, K. Keck and S. H. Selman (1992) Observations on the synthesis and in vivo photodynamic activity of some benzochlorins. *Photochem. Photobiol.* **55**, 133–136.
10. Morgan, A. R., G. M., Garbo, R. W. Keck and S. H. Selman (1988) New photosensitizers for photodynamic therapy: combined effect of metallopurpurin derivatives and light on transplantable bladder tumors. *Cancer Res.* **48**, 194–198.
11. Zheng, G., W. R. Potter, A. Sumlin, T. J. Dougherty and J. R. K. Pandey (2000) Photosensitizers related to purpurin-18_N-alkylimides. A Comparative in vivo tumoricidal ability of ester vs amide functionalities. *Bioorg. Med. Chem. Lett.* **10**, 123–127.
12. Kozyrev, A. K., G. Zheng, T. J. Dougherty, K. M. Smith and R. K. Pandey (1996) Syntheses of stable bacteriochlorophyll-a derivatives as potential photosensitizers for PDT. *Tetrahedron Lett.* **37**, 6431–6434.
13. Pandey, R. K., A. Sumlin, F-Y. Shiau, T. J. Dougherty and K. M. Smith (1992) Structure activity relationships among photosensitizers related to pheophorbides and bacteriopheophorbides. *Bio-org. Med. Chem. Lett.* **2**, 491–494.
14. MacDonald, I. J. and T. J. Dougherty (2001) Basic principles of photodynamic therapy. *J. Porphyrins and Phthalocyanines* **5**, 105–129.
15. Osterloh, J. and M. G. H. Vicente (2002) Mechanisms of porphyrinoid localization in tumors. *J. Porphyrins and Phthalocyanines* **6**, 305–324.
16. Pandey, R. K., D. A. Bellnier, K. M. Smith and T. J. Dougherty (1991) Porphyrin and chlorin derivatives as potential photosensitizers in photodynamic therapy. *Photochem. Photobiol.* **53**, 65–72.
17. Henderson, B. W., D. A. Bellnier, W. R. Greco, A. Sharma, R. K. Pandey, L. Vaughan, K. R. Weishaupt and T. J. Dougherty (1997) A quantitative structure-activity relationship for a congeneric series of pyropheophorbide derivatives as photosensitizers for photodynamic therapy. *Cancer Res.* **57**, 4000–4007.
18. Zheng, G., S. Camacho, W. Potter, D. A. Bellnier, B. W. Henderson, T. J. Dougherty and R. K. Pandey (2001) Synthesis, tumor uptake and invivo photosensitizing efficacy of a homologous series of the 3-(1′-alkoloxy)ethyl-purpurin-18-N-alkylimides. *J. Med. Chem.* **44**, 1540–1559.
19. Li, G., A. Graham, Y. Chen, M. P. Dobhal, J. Morgan, G. Zheng, A. Kozyrev, A. Oseroff, T. J. Dougherty and R. K. Pandey (2003) Synthesis, comparative photosensitizing efficacy, human serum albumin (Site II) binding ability, and intracellular localization characteristics of novel benzobacteriochlorins derived from *vic*-dihydroxybacteriochlorins. *J. Med. Chem.* **46**, 5349–5359.
20. Chen, Y. H., A. Graham, W. R. Potter, J. Morgan, L. Vaughan, D. A. Bellnier, B. W. Henderson, A. Oseroff, T. J. Dougherty and R. K. Pandey (2002) Bacteriopurpurinimides: highly stable and potent photosensitizers for photodynamic therapy. *J. Med. Chem.* **45**, 255–258.
21. Vakrat-Hogalili, Y., L. Weiner, V. Brumfield, A. Brandis, Y. Saloman, B. McIlroy, B. C. Wilson, A. Pawlak, M. Rozanowska, T. Sarna and A. Scherz (2005) The microenvironment effect on the generation of reactive oxygen species by Pd-bacteriochloropheophorbide. *J. Am. Chem. Soc.* **127**, 6489–6497.
22. Finley, J. C., S. Mitra and T. H. Foster (2002) In vivo m-THPC photobleaching in normal rat skin exhibits unique irradiance dependent features. *Photochem. Photobiol.* **75**, 282–288.
23. Kessel, D. and Y. Luo (1999) Mitochondrial photodamage and PDT induced apoptosis. *Cell. Differ.* **6**, 28–35.
24. Kessel, D., Y. Luo, Y. Deng and C. K. Chang (1997) The role of subcellular localization in inhibition of apoptosis by photodynamic therapy. *Photochem. Photobiol.* **65**, 422–426.
25. Kessel, D., M. Antolovich and K. M. Smith (2001) The role of the peripheral benzodiazepine receptor in the apoptotic response to photodynamic activity. *Photochem. Photobiol.* **74**, 346–349.
26. Moan, J., K. Berg, A. Anholt and K. Madslien (1994) Sulfonated aluminum phthalocyanines as sensitizers for photochemotherapy. Effects of small doses on localization, dye fluorescence and photosensitivity in V79 cells. *Int. J. Cancer.* **58**, 865–870.
27. Morgan, J., W. R. Potter and A. R. Oseroff (2000) Comparison of photodynamic targets in a carcinoma cell line and its mitochondrial DNA–deficient derivative. *Photochem. Photobiol.* **70**, 747–757.
28. MacDonald, I. J., J. Morgan, D. A. Bellnier, G. M. Paszkiewicz, J. E. Whitaker, D. A. Litchfield and T. J. Dougherty (1999) Subcellular localization pattern and their relationship to photodynamic activity of pyropheophorbide-a derivatives. *Photochem. Photobiol.* **70**, 789–797.
29. Rungta, A., G. Zheng, J. R. Missert, W. R. Potter, T. J. Dougherty and R. K. Pandey (2000) Purpurinimides as photosensitizers: effect of the presence and position of the substituents in *in vivo* photodynamic efficacy. *Bioorg. Med. Chem. Lett.* **10**, 1463–1466.
30. Pandey, R. K., S. Constantine, D. A. Goff, A. Kozyrev, T. J. Dougherty and K. M. Smith. (1996) Chlorophyll-a derivatives as photosensitizers for photodynamic therapy: effect of the position of n-

heptyl ether side chain in *in vivo* photosensitizing efficacy. *Bioorg. Med. Chem. Lett.* **6**, 105–110.
31. Jaquinod, L., D. J. Nurco, C. J. Medforth, R. K. Pandey, T. P. Forsyth, M. M. Olmstead and K. M. Smith (1996) Synthesis and characterization of bis(chlorines) from McMurry reaction of formylchlorins. *Angew. Chem.* **35**, 1013–1015.
32. Kozyrev, A. N., V. Suresh, S. Das, M. O. Senge, M. Shibata, T. J. Dougherty and R. K. Pandey (2000) Syntheses and spectroscopic studies of novel chlorins with fused quinoxaline or benzimadazole ring systems and the related dimers with extended conjugation. *Tetrahedron* **56**, 3353–3364.
33. Magde, D. R., R. Wong and P. G. Seybold (2002) Fluorescence quantum yields and their relation to lifetimes of rhodamine B and fluorescein in nine solvents: improved absolute standards for quantum yields. *Photochem. Photobiol.* **75**, 327–334.
34. Demas, J. N., E. W. Harris and R. P. McBride (1977) Energy transfer from luminescent transition metal complexes to oxygen. *J. Amer. Chem. Soc.* **99**, 3547–3551.
35. Kalsi, P. S. (1993) *Spectroscopy of Organic Compounds*, pp. 7–58. Wiley Eastern Limited, New Delhi.
36. Kalsi, P. S., K. R. Schwartz, M. C. G. Aalders and J. B. Dankert (2005) Photodynamic inactivation of fibroblasts by a cationic porphyrin. *Laser Med. Sci.* **20**, 62–67.
37. Almeida, R.D., B. J. Manadas, A. P. Carvalho and C. B. Duart (2004) Intracellular signaling mechanisms in photodynamic therapy. *Biochim. Biophys. Acta* **2**, 59–86.
38. Pagano, R. E., O. C. Martin, H. C. Kang and R. P. Haughland (1991) A novel fluorescent ceramide analogue for studying membrane traffic in animal cells: accumulation at the Golgi apparatus results in altered spectral properties of the sphingolipid precursor. *JCB* **113**, 1267–79.
39. Kozyrev, A. N., T. J. Dougherty and R. K. Pandey (1998) LiOH-promoted allomerization of pyropheophorbide-a. A convenient synthesis of 13^2-oxopyropheophorbide-a and its unusual enolization. *Chem. Commun.* **4**, 481–482.
40. Chen, Y., X. Zheng, M. P. Dobhal, A. Gryshuk, J. Morgan, T. J. Dougherty, A. Oseroff and R. K. Pandey (2005) Methyl pyropheophorbide-a analogous: potential fluorescent probes for the peripheral-type benzodiazepine receptor. Effect of central metal in photosensitizing efficacy. *J. Med. Chem.* **48**, 3692–3695.
41. Harriman, A. (1980) Luminescence of porphyrins and metalloporphyrins. Part 1. – Zinc(II), nickel(II) and manganese(II) porphyrins. *J. Chem. Soc. Faraday Trans. I* **76**, 1978–1985.
42. Harriman, A. (1981) Luminescence of porphyrins and metalloporphyrins. Part 3. Heavy-atom effects. *J. Chem. Soc., Faraday Trans. 2* **77**, 1281–1291
43. Rubio, N., P. Prat, N. Bou, J. I. Borrell, J. Teixidó, Á. Villanueva, Á. Juarranz, M. Cañete, J. C. Stockert and S. Nonell (2005) A comparison between the photophysical and photosensitising properties of tetraphenyl porphycenes and porphyrins. *New J. Chem.* **29**, 378–384
44. Valicsek Z., O. Horvat and K. L. Stevenson (2004) Photophysics and photochemistry of water-soluble, sitting-atop bis-thallium(I) 5,10,15,20-tetrakis(4-sulfonatophenyl) porphyrin. *Photochem. Photobiol. Sci.* **3**, 669–73.
45. Azenha, E. G., A. C. Serra, M. Pineiro, M. M. Pereira, J. S. de Melo, L. G. Arnaut, S. J. Formosinho and A. M. d'A. R. Gonsalves (2002) Heavy-atom effects on metalloporphyrins and polyhalogenated porphyrins. *Chem. Phys.* **280**, 177–190.
46. Zenkevich E, E. Sagun, V. Knyukshto, A. Shulga, A. Mironov, O. R. Efremova, R. Bonnett, S. P. Songca and M. Kassem (1996) Photophysical and photochemical properties of potential porphyrin and chlorin photosensitizers for PDT. *J. Photochem. Photobiol. B* **33**, 171–180.
47. Yagai, S. and H. Tamiaki (2001) Synthesis and self-aggregation of zinc chlorophylls possessing an ω-hydroxyalkyl group: effect of distance between interactive hydroxy group and chlorin moiety on aggregation. *J. Chem. Soc., Perkin Trans. 1* **23**, 3135–3144.